

1.A Study on D0 Run2b Stave Structural Performance

Giobatta Lanfranco

*Fermi National Accelerator Laboratory
Particle Physics Division / Silicon Engineering Group - Mechanical Dep.
e-mail: giobatta@fnal.gov*

30 April 2002

1. Abstract

Two different structural solutions have been proposed and studied for the D0 Run2b stave (Figure 1 and Figure 3). The way the stave structural stiffness is achieved in both designs is essentially the same: the structural material is displaced as far as possible from the neutral axis in order to increase the bending moment of the stave.

The agreement of the measured data with what has been theoretically predicted is excellent. The C channel stave with dog-bones glued on top of the sensor (stave #2) has outperformed the other mockups with a predicted sag of 51 μ m for a distributed load of 2.28 N/m [0.013 lbf/in] and a consequent natural frequency of 89.2Hz. The other three C channel staves with the dog-bones not glued on the sensor have a bending stiffness that is -19.0%, -10.8%, +4.0% of that of stave #2, being 11.0%, 7.8%, 15.1% lighter respectively.

An optimized stave structural proposal with 130.5% of the design stiffness within the mass budget is presented at the end of this paper.

2. The two stave layouts

The first stave design (Figure 1) is obtained enclosing the entire stave core between two carbon fiber shells presenting 20.2mm \times 6.2mm cut-outs to allow the cables to be plugged in the hybrid connectors. The initial advantage that this solution seems to offer in terms of wirebonds protection is penalized by the significant local deformations that the thin shells are subject to when an external load is applied¹.

¹ In Figure 2 it is possible to see the finite element study on the effects of a concentrated 100 grams load on the shell local deformation.

Besides, the part of shell that effectively takes part in the structural stiffness is reduced by the width of the holes, and this consequently translates in a waste of material. This approach has also the disadvantage that the shear stresses between the upper and bottom flanges are carried through a weak web (because of the glue seam between the two shells) and it is not clear how the assembly process can be easily achieved. However, with this design the shells are glued on the core with a top-down movement, making the installation less critical for the wirebonds integrity. Two of the existing mockups follow this design and in Figure 7 and Figure 11 the deflection test results are shown.

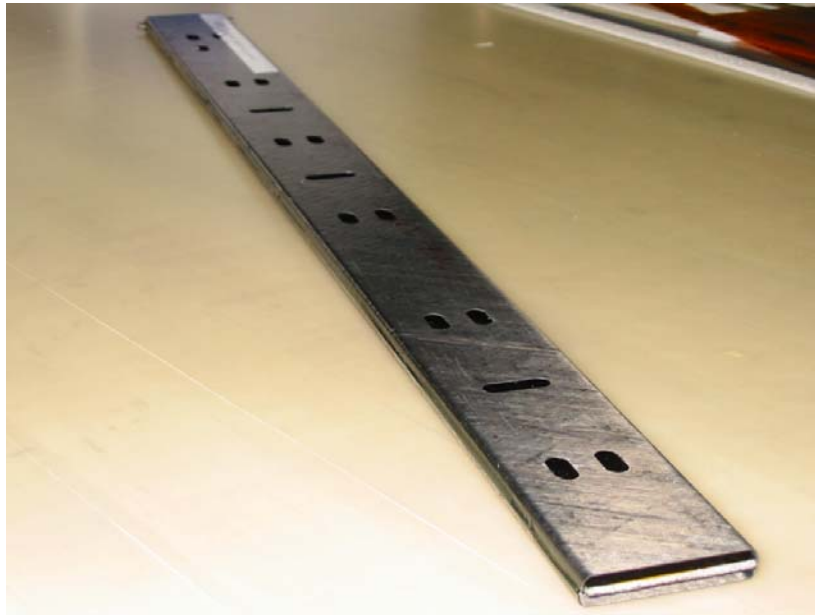


Figure 1 – The stave mockup with outer shell solution. Stave #4.

Figure 3 it is possible to see an enlarged view of a stave with Kevlar skin core and the alignment pins at $z = 610\text{mm}$.

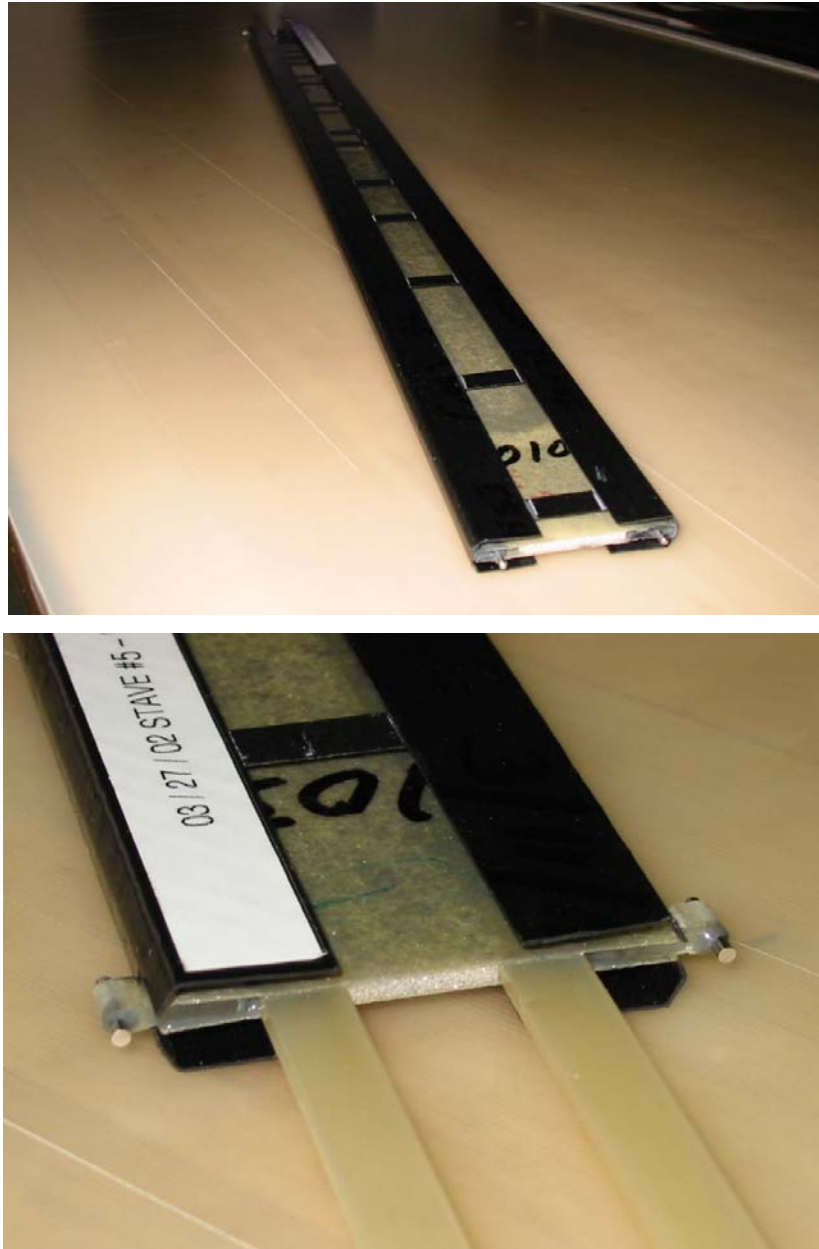


Figure 3– The stave mockup with C channels configuration and close-up of the alignment pins region at $z = 610\text{mm}$. The rectangular shaped PEEK cooling line is also visible. Stave #5.

The C channel section (Figure 4) has been optimized to provide the best compromise between bending stiffness and compact profile⁴.

⁴ to reduce the insertion cut-out in the bulkhead at $z = 610\text{mm}$.

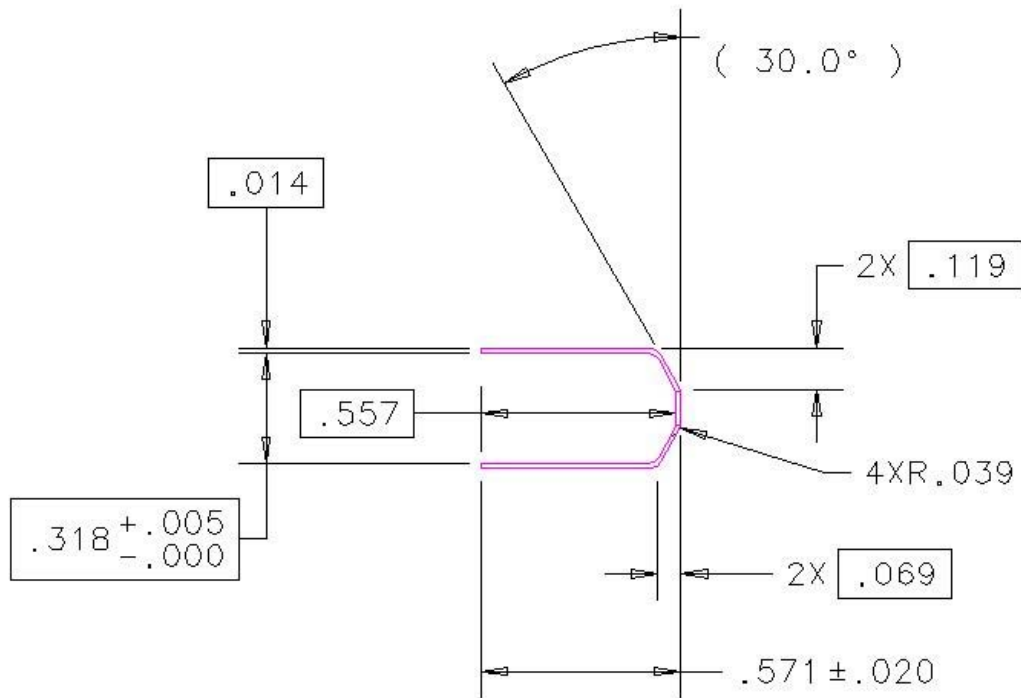


Figure 4 – Optimized C channel profile.

Figure 5 illustrates a kapton skin core before the C channels are glued along the sides.

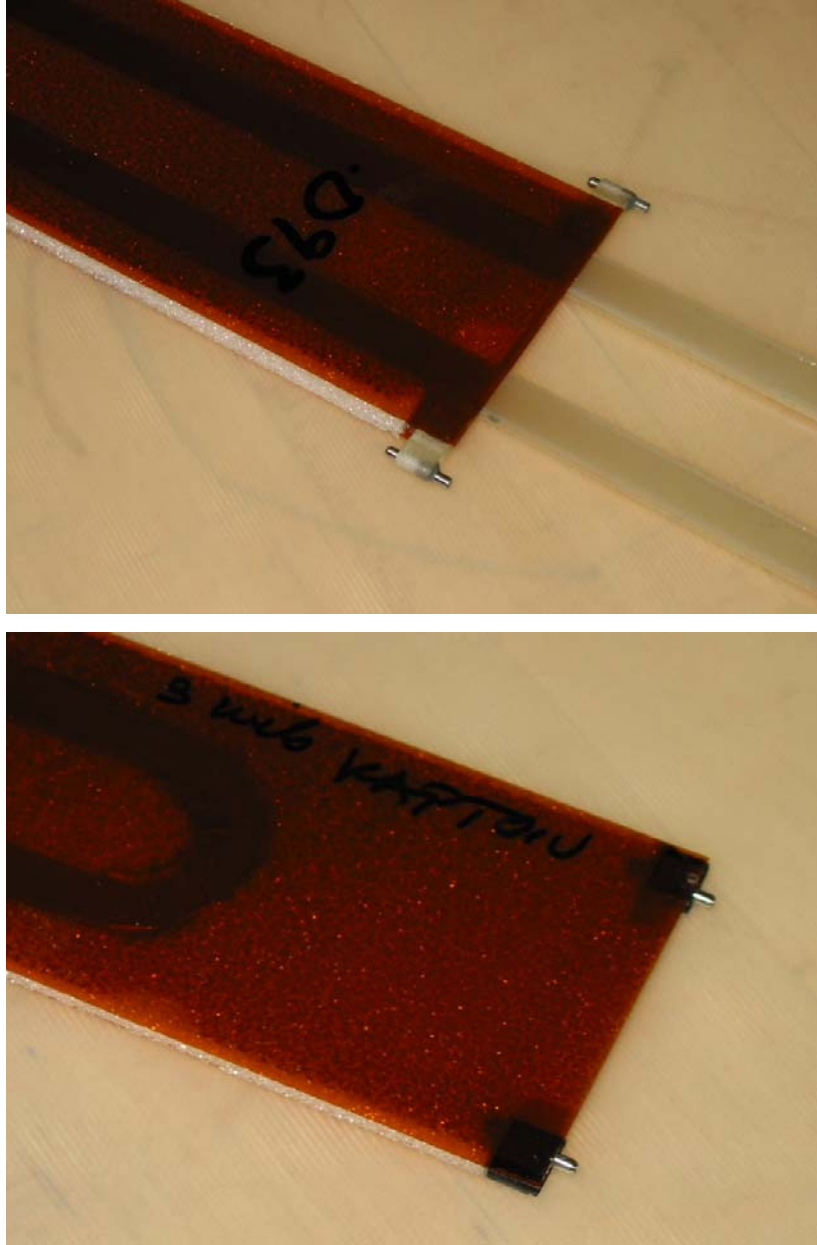


Figure 5 – Core detail with kapton skin and alignment pins. Top: $z = 609.6\text{mm}$ end; bottom: $z = 0\text{mm}$ end.

Figure 8 through Figure 13 show the results of deflection test of this stave design. For the current tests no silicon sensors have been glued on top of the cores.

3. Test description

The estimated distributed load that is supposed to be carried by the stave is about 2.28 N/m (0.013 lb/in), and it is due to the weight of the silicon sensors, the hybrids, the cabling, the coolant and the supporting structure itself. In these conditions the stave maximum allowed vertical displacement is

60 μ m which yields a target bending stiffness of 68.228Pa \times m⁴ from which it is possible to draw the design goal line of Figure 7 through Figure 13 (dashed blue line).

The test has been performed placing the stave on two end supports and loading the center of the stave while a dial indicator was registering the deflection (Figure 6). The dial indicator stylus was positioned on one of the two upper flanges for the channel design, given their intrinsic local rigidity; for the shell design, the stylus was placed on a pin glued on the core (stave #0), to directly measure the core deflection, or on the lower and on the upper shell (stave #4), to compare the effect of the local deformation.

The load test has been repeated with the stave flipped to load it in the opposite direction in order to compare possible deflection discrepancy. No differences have been noticed except for stave #4 (Figure 11), but this can be explained by the fact that the two shells were not perfectly matching at their interface.



Figure 6 – Setup of the deflection test.

4. Results

The agreement of the measured data with theoretical prediction is excellent. Except stave #1 (Figure 8) because of the aluminum sheet in the lay-up, all the mockups based on the channel configuration

performed within or close to the design specifications. The dog-bones glued on top of the sensors offer a slight increase in bending stiffness at the cost of about 7 grams of extra mass⁵.

In staves #2 and #3 the first and last longitudinal plies of the lay-up have been applied only along the flanges and not along the web (to highlight this in the following graphs a * designates the partial ply); although there is a modest gain in mass (~2 grams), the additional lay-up labour⁶ does not justify this solution.

The design differences between the six stave mockups, together with their overall mass, the predicted sag under the estimated distributed load of 0.013lb/in and the stave bending stiffness have been summarized in Table 2.

The formula

$$f = \frac{1.2769}{2\pi} \sqrt{\frac{g}{\delta_{\max}}}$$

Equation 1

where g is the gravitational acceleration and δ_{\max} the maximum sag, represents a simple but close approximation for the fundamental frequency of a uniform thin plate of ordinary shape having any combination of fixed, partially fixed or simply supported boundaries (Ref. 1). Having imposed that the sag does not exceed 60 μ m implies that the natural frequency of the stave will never be lower than about 80Hz, reducing then the danger of 60Hz resonance. In Table 2 the natural frequency of the tested mockup staves is given, based on the expected sag due to the estimated overall stave mass (~140gr).

Finally, a pronounced creep has been observed in stave #1 (channel design) and in staves #0 and #4 (the two shell mockups). About the former stave, this could be explained by the presence of the aluminum in the lay-up, the only substantial difference with the other models based on the same design.

⁵ The estimated total stave mass is 144.75gr, 45.8gr of which is the predicted mass of the structure. At the present time, stave #6 is the lightest structure built (61.81gr) but it is still 16gr beyond what is expected, pointing out the necessity to improve the control of the glue thickness.

⁶ During the lay-up procedure, the first two longitudinal prepreg strips are directly applied on the mold; then the first set of [$\pm 60^\circ / 0^\circ$] plies, previously stacked up together and containing the only complete longitudinal ply, are wrapped around the mold; then the next [$\pm 60^\circ$], previously stacked too. After partial curing, the final two longitudinal prepreg strips are applied and the channel undergoes a final curing step. This extra step is determined by the difficulty to precisely place the two strips in case they were stacked on the last [$\pm 60^\circ$] set before being wrapped around the mold.

The creep in the shell staves, as already pointed out, could be due to the fact that the shear stresses along the web are carried through the weak epoxy seam keeping the shells together.

Stave #0 (Shell) Deflection - [0° / 0° / 90° / 0° / 0°]
stave weight = 72.42 gr / glue: DP-190

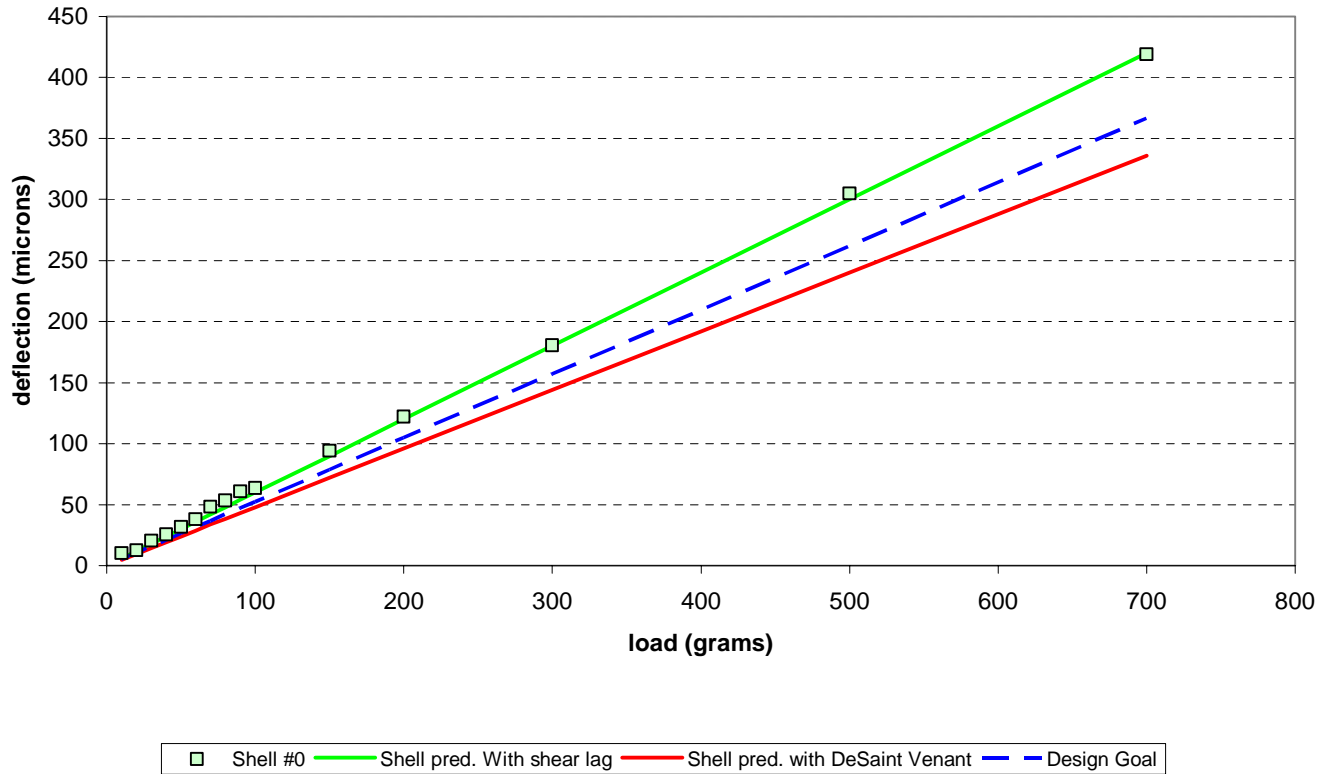


Figure 7 - Stave #0 mockup deflection study. The shell structural elements are made of carbon fiber prepreg (Mitsubishi K139, [0°, 0°, 90°, 0°, 0°]). The core is made of Rohacell, 200µm thick carbon skin and 50µm thick Kapton. This model is about 0.5 inch shorter than the final design goal and 1.2 mm taller (overall stave height: 10.00mm). The shear lag theory correctly predicts the behavior of this thin wall structure while the De Saint Venant theory fails. The design goal line has been opportunely adjusted by a $(8.8/10)^2$ scale factor to account for the extra height of this stave.

Stave #1 Deflection - [0° / ±45° / Al foil / ±45° / 0°]
15mm dogbones glued on top of sensor - stave weight = 77.60 gr / glue: DP-190

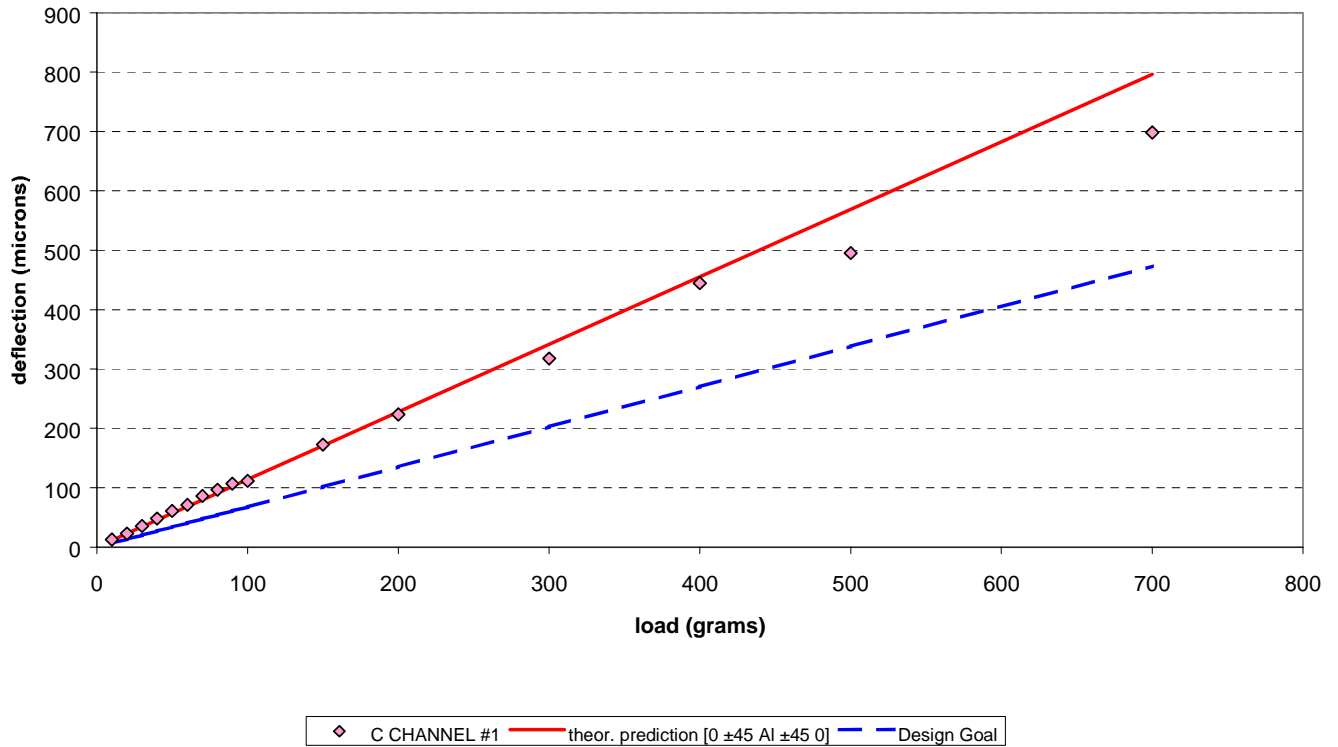


Figure 8 – Stave #1 mockup deflection study. The 15 mm wide dog-bones (wirebonds protections) are glued on top of the silicon sensors. The C channel structural elements are ~13.2mm wide × ~9.0mm tall and made of carbon fiber prepreg (Mitsubishi K139, [0°, ±45°] lay-up) with interposed a 1 mil aluminum sheet. The core is made of Rohacell, 200µm thick carbon skin and 50µm thick Kapton.

Stave #2 Deflection - $[0^\circ * / \pm 60^\circ / 0^\circ / \pm 60^\circ / 0^\circ *]$
7.5mm dogbones glued on top of sensor - stave weight = 72.79 gr / glue: DP-190

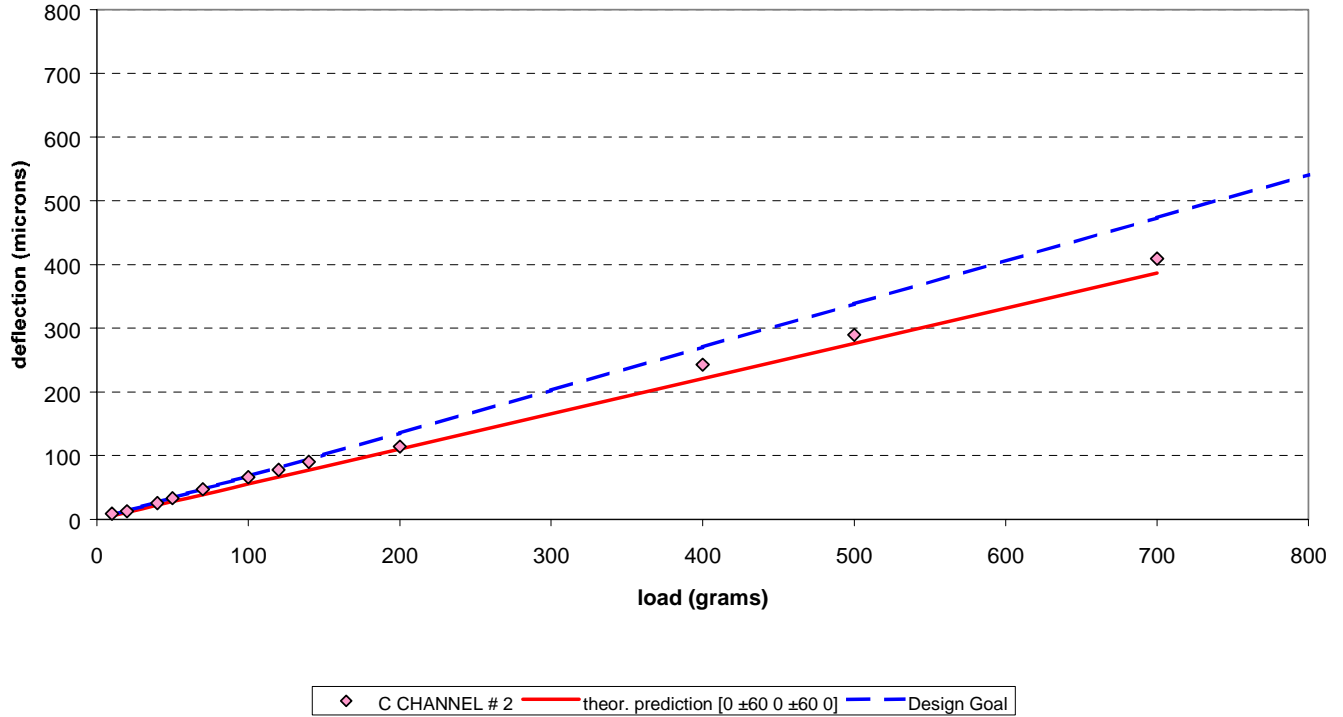


Figure 9 - Stave #2 mockup deflection study. The dog-bones are still glued on top of the silicon sensor but now their width has been reduced to 7.5mm. The C channel width has been increased to ~15.7mm × 9.2mm tall and the carbon fiber (Mitsubishi K139) 7 plies lay-up is now $[0^\circ, \pm 60]$ (the aluminum sheet has been replaced with a longitudinal lamina and the outer longitudinal plies are only on the flanges). The core is made of Rohacell, 200µm thick carbon skin and 50µm thick kapton.

Stave #3 Deflection - [0° * / ±60° / 0° / ±60° / 0° *]
dogbones glued on flanges only - stave weight = 64.77 gr / glue: DP-190

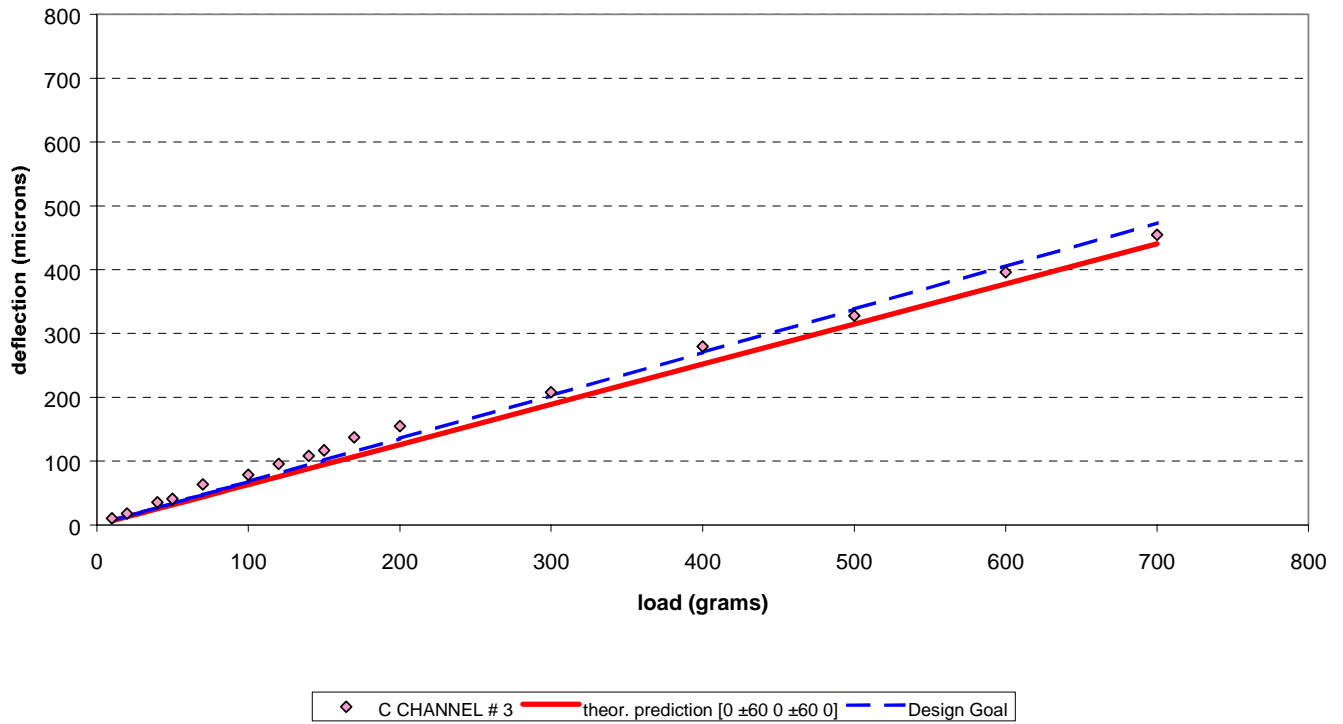


Figure 10 - Stave #3 mockup deflection study. The dog-bones are reduced to carbon sheets (7.5mm wide × 200µm thick). The C channels are analogous to that of the stave #2 (Mitsubishi K139 [0°, ±60°, 0°, ±60°, 0°] lay-up, outer longitudinal plies only on the flanges, overall height 9.20mm). The core is made of Rohacell, 200µm thick carbon skin and 50µm thick Kapton.

Stave # 4 (Shell) Deflection - [0° / -°60 / +°60 / +°60 / -60° / 0°]
 stave weight = 65.86 gr / glue: DP-190

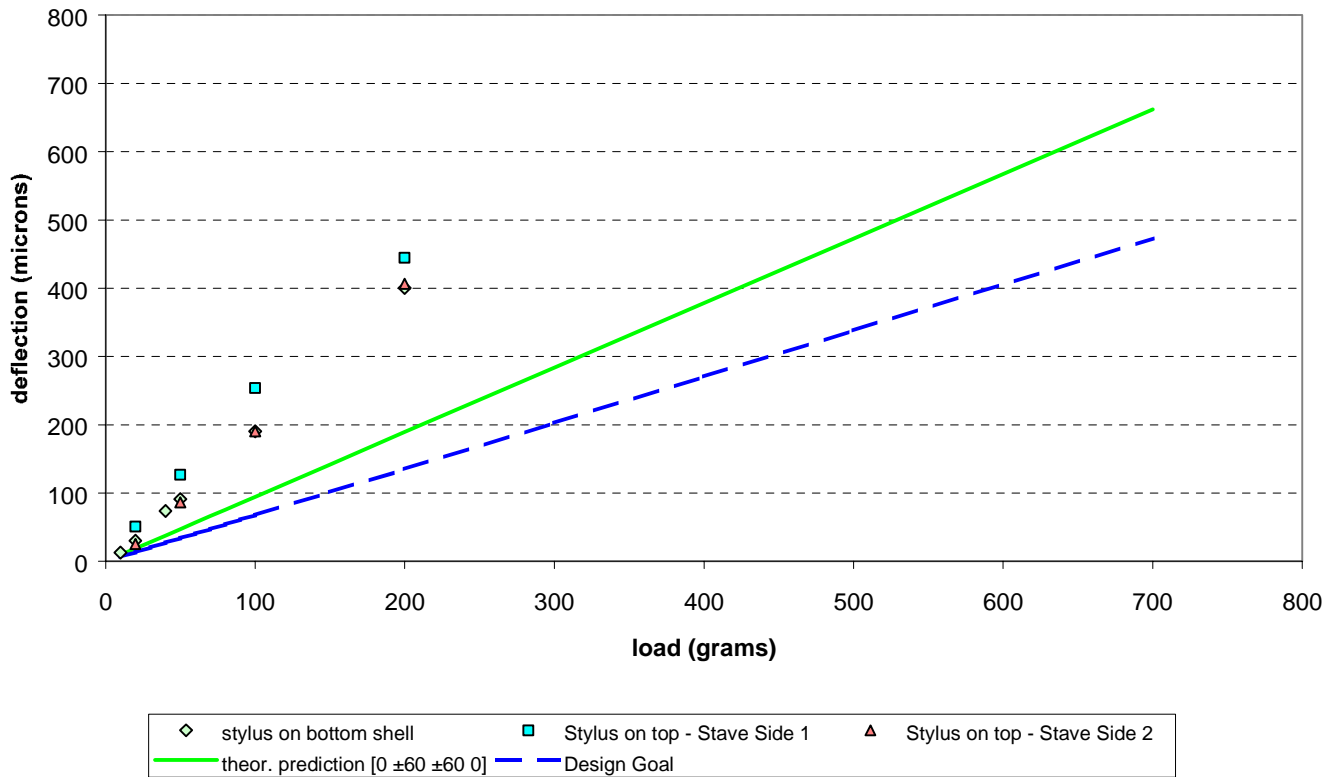


Figure 11 – Stave #4 mockup deflection study. The shell structural elements are made of carbon fiber prepreg (Mitsubishi K139, 6 plies [0°, ±60, ±60°, 0°] lay-up). The core is made of Rohacell, 200µm thick carbon skin and 50µm thick Kapton. The data points refer to the different locations of the dial indicator stylus. The geometrical differences between the shells are likely to cause the sag discrepancy between the two sides of the stave. Problems with the glue seam between the shells can probably explain the poor performance of this stave.

Stave #5 Deflection - [0° / ±45° / 0° / ±45° / 0°]
dogbones glued on flanges only - stave weight = 67.10 gr / glue: DP-190

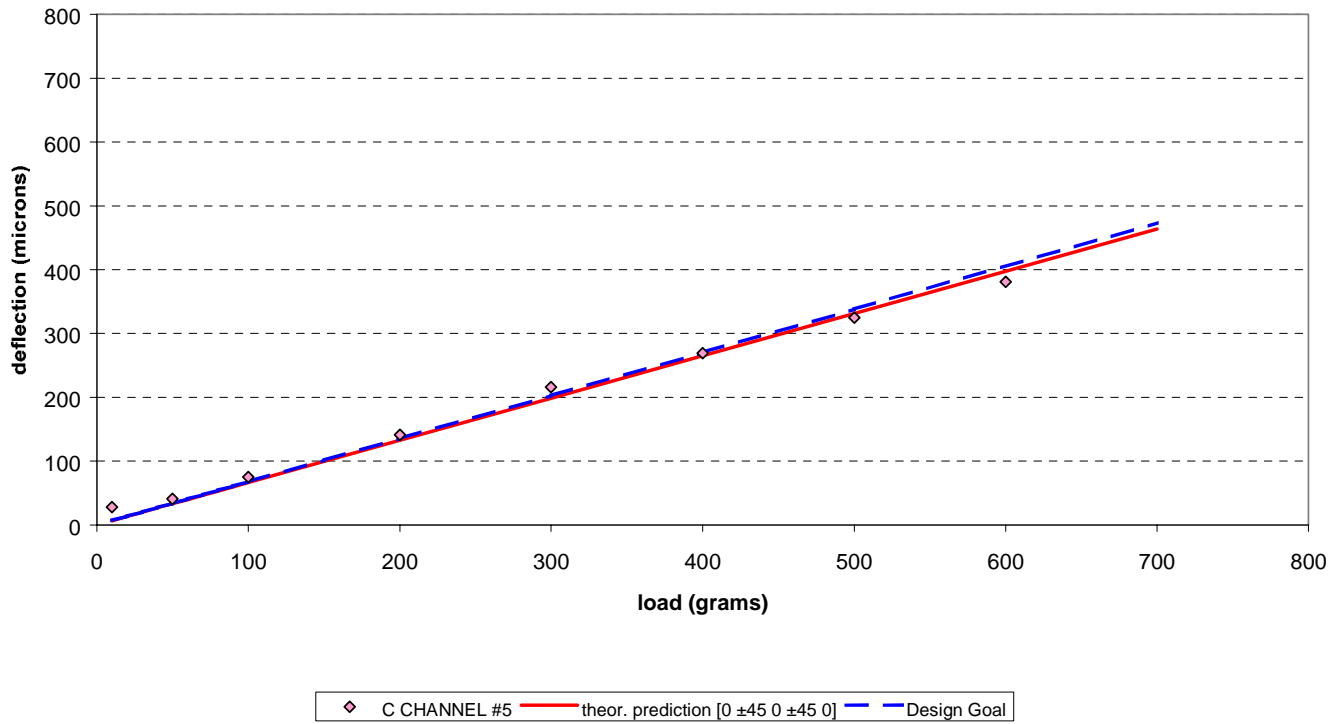


Figure 12 - Stave #5 mockup deflection study. The only structural difference between this model and stave #3 is in the C channel fiber lay-up (Mitsubishi K139 [0° / ±45]). This contributes slightly to the bending stiffness of the structure, although the lesser stave overall height (~8.71mm vs the 9.20mm) counteracts this. The core is made of Rohacell and 6 mils thick Kevlar.

Stave #6 Deflection - [0° / ±45° / 0° / ±45° / 0°]
dogbones glued on flanges only - stave weight = 61.81 gr / glue: DP-190

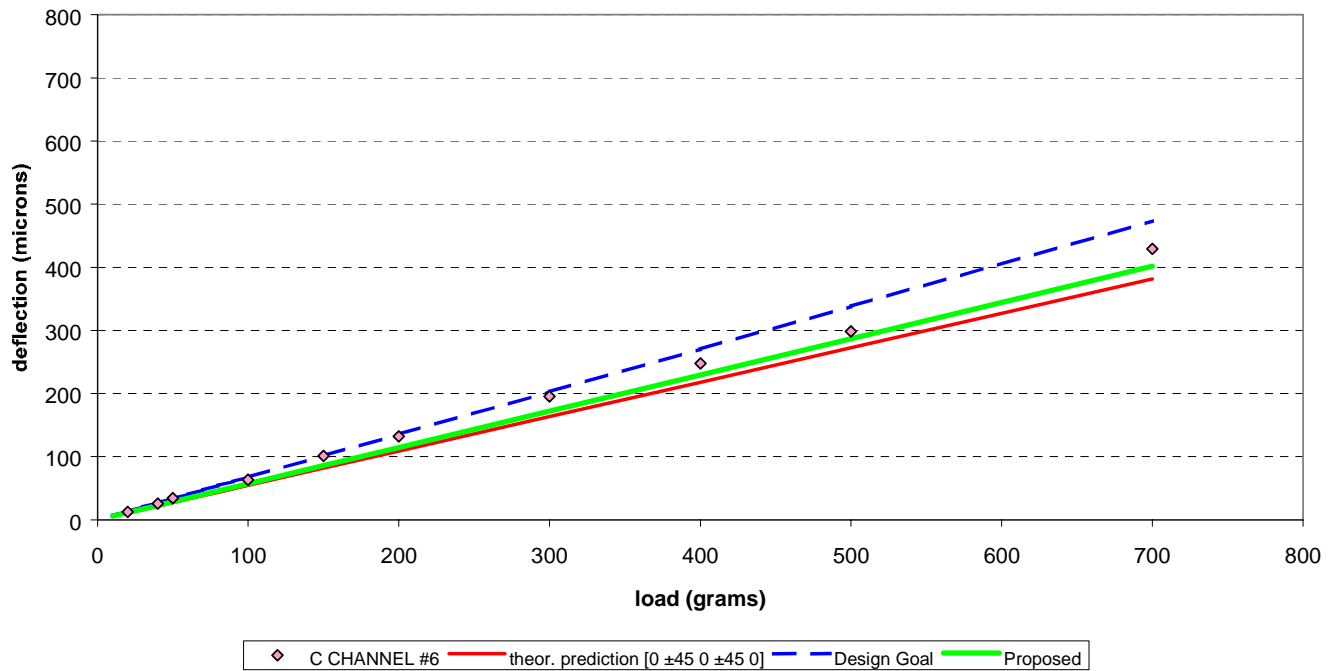


Figure 13 – Stave #6 mockup deflection study. Similar to stave #5 but with fiberglass skin core about 3 mils thick. The green line shows how the channel structure with the proposed lay-up is expected to perform.

The figure of merit (*FM*) reported in the last column of Table 2 provides a quick way to compare the different mockups analyzed so far. It is calculated using the following relation

$$FM = \frac{60\mu m}{\text{calculated_sag}} \times \frac{(8.8mm - \text{goal_wall_thickness})^2}{(\text{measured_mockup_height} - \text{measured_wall_thickness})^2}$$

Equation 2

60µm being the goal maximum sag, 8.8mm the overall stave height, and the goal wall thickness is 250µm for the shell design and 360µm for the channel configuration. Since according to Equation 2 values of *FM* greater than 1 indicate a design performing better than our goal, it follows that only the channel solution is capable of meeting the specified requirements of stiffness, with stave #6 being the best performer.

5. Channel development

The actual channel can be further improved adopting a thinner ply with a less resin rich prepreg. This has the double advantage to increase the laminate bending stiffness and reduce the wall thickness (allowing extra safe space for the wirebonds).

Table 1 shows the properties of a laminate made with a K139/EX1515 lamina (Mitsubishi K139 fiber – 55gsm fiber areal weight, 45µm ply thickness – with 29.3% by mass EX1515 resin⁷) and the following 8 plies lay-up: [0°, ±45°, 0°, 0°, ±45°, 0°].

Ex (pa)	2.21E+11	Ex (psi)	3.20E+07
Ey (pa)	4.87E+10	Ey (psi)	7.06E+06
Ez (pa)	6.30E+09	Ez (psi)	9.13E+05
Gxy (pa)	5.54E+10	Gxy (psi)	8.03E+06
Gxz (pa)	3.93E+09	Gxz (psi)	5.69E+05
Gyz (pa)	2.98E+09	Gyz (psi)	4.33E+05
NUxy	8.84E-01	NUxy	8.84E-01
NUyx	1.95E-01	NUyx	1.95E-01
NUxz	7.89E-03	NUxz	7.89E-03
NUzx	2.25E-04	NUzx	2.25E-04
NUyz	2.07E-01	NUyz	2.07E-01
NUzy	2.67E-02	NUzy	2.67E-02
CTEx	-1.42E-06	CTEx (in/in/F)	-7.90E-07
CTEy	1.50E-06	CTEy (in/in/F)	8.32E-07
CTEz	3.67E-05	CTEz (in/in/F)	2.04E-05
CTEyz	0.00E+00	CTEyz (in/in/F)	0.00E+00
CTEzx	0.00E+00	CTEzx (in/in/F)	0.00E+00
CTExy	-4.49E-22	CTExy (in/in/F)	0.00E+00
CME _x	-2.34E-05	CME _x	-2.34E-05
CME _y	1.85E-03	CME _y	1.85E-03
CME _z	2.44E-02	CME _z	2.44E-02
CME _{yz}	0.00E+00	CME _{yz}	0.00E+00
CME _{zx}	0.00E+00	CME _{zx}	0.00E+00
CME _{xy}	-2.80E-19	CME _{xy}	0.00E+00
K _x (W/m/K)	8.95E+01	K _x (Btu/hr/ft/F)	5.17E+01
K _y (W/m/K)	3.01E+01	K _y (Btu/hr/ft/F)	1.74E+01
K _z (W/m/K)	3.23E-01	K _z (Btu/hr/ft/F)	1.87E-01
K _{xy} (W/m/K)	5.85E-16	K _{xy}	-1.26E-17
Den (g/m ³)	1.73E+06	Den (lb/in ³)	6.24E-02
Thick (mm)	3.60E-01	Thick (in)	1.42E-02

Table 1 – Laminate properties for K139 fiber with 30% mass RS-12 polycyanate resin and [0° / ±45° / 0° / 0° / ±45° / 0°] lay-up.

⁷ EX1515 is a 225–250° F cure toughened cyanate resin for spacecraft and other cryogenic applications that require temperature stable structures.

The use of such a laminate to build a 8.8mm high \times 14.5mm wide channel would give a predicted bending moment of $120m^4 \times Pa$, which is a 76% gain from the design goal. This yields $34\mu m$ sag under the 0.013lb/in load and a 109Hz fundamental frequency for the structure. In this case the figure of merit would be 1.76.

Stave #	Design	shell / channel w [mm] \times h [mm]	lay-up	lay-up thckns [μm]	stave mass [gr]	EI [$m^4 \times Pa$]	sag @ 0.013lb /in [μm]	f [Hz]	FM
0	shell [small cut-outs] ! TOO TALL!	47.2 \times 10.0	0° / 0° / 90° / 0° / 0°	300	72.42	77	53	87	0.88
1	C channel [15mm wide dog-bones glued on Si]	13.2 \times 8.9	0° / $\pm 45^\circ$ / Al / $\pm 45^\circ$ / 0°	350	77.60	41	101	63	0.60
2	C channel [7.5mm wide dog-bones glued on Si]	15.6 \times 9.1	0° * / $\pm 60^\circ$ / 0° / $\pm 60^\circ$ / 0° *	480	72.79	84	49	91	1.23
3	C channel [7.5mm wide dog-bones NOT on Si]	15.4 \times 9.2	0° * / $\pm 60^\circ$ / 0° / $\pm 60^\circ$ / 0° *	410	64.77	74	56	85	1.08
4	shell [final cut-outs layout]	46.7 \times 8.75	0° / $\pm 60^\circ$ / $\pm 60^\circ$ / 0°	250	65.86	25	162	50	0.37
5	C channel [7.5mm wide dog-bones NOT on Si – Kevlar skin core]	15.5 \times 8.72 ⁸	0° / $\pm 45^\circ$ / 0° / $\pm 45^\circ$ / 0°	420 ⁸	67.10	70	59	83	1.02
6	C channel [7.5mm wide dog-bones NOT on Si – Fiberglass skin]	15.35 \times 9.13 ⁸	0° / $\pm 45^\circ$ / 0° / $\pm 45^\circ$ / 0°	476 ⁸	61.81	85	48	92	1.24
*	Proposed prepreg lay-up C channel	14.5 \times 8.8	0° / $\pm 45^\circ$ / 0° / 0° / $\pm 45^\circ$ / 0°	360	45.8	81	51	89	1.18

Table 2 – Summary of the stave mockups characteristics: stave design, dimensions of the adopted structural solution, prepreg lay-up, stave mass, bending stiffness, estimated sag for the expected distributed load, stave fundamental frequency, figure of merit. The figure of merit (FM) reported in the last column provides a quick way to compare the different mockups analyzed so far (the higher the better; a design with FM less than 1 does not meet the specified requirements of stiffness).

⁸ CMM measurement.

6 . References

1. «Roark's Formulas for stress and strain», W.C. Young, R.G. Budynas, 7th ed., McGraw Hill